



## Modeling and Validation of 48 V Mild Hybrid Lithium-Ion Battery Pack

SoDuk Lee, Jeff Cherry, Michael Safoutin, Joseph McDonald, and Michael Olechiw U.S. Environmental Protection Agency

**Citation:** Lee, S.D., Cherry, J., Safoutin, M., McDonald, J. et al., "Modeling and Validation of 48 V Mild Hybrid Lithium-Ion Battery Pack," SAE Technical Paper 2018-01-0433, 2018, doi:10.4271/2018-01-0433.

### Abstract

As part of the Midterm Evaluation of the 2017-2025 Light-duty Vehicle Greenhouse Gas (GHG) Standards, the U.S. Environmental Protection Agency (EPA) developed simulation models for studying the effectiveness of the 48 V mild hybrid technology for reducing CO<sub>2</sub> emissions from light-duty vehicles. Simulation and modeling of this technology requires a suitable model of the battery. This paper presents the development and validation of a 48 V lithium-ion battery model that will be integrated into EPA's ALPHA vehicle simulation model and that can also be used within Gamma Technologies, LLC (Westmont, IL) GT-DRIVE™ vehicle simulations. The battery model is a standard equivalent circuit model with two-time constant resistance-capacitance (RC) blocks. Resistances and capacitances were calculated using test data from an 8 Ah, 0.4 kWh, 48 V (nominal) lithium-ion battery obtained from a Tier 1 automotive supplier, A123 Systems, and developed specifically for 48 V mild hybrid

vehicle applications. The A123 Systems battery has 14 pouch-type lithium ion cells arranged in a 14 series and 1 parallel (14S1P) configuration. The RC battery model was validated using battery test data generated by a hardware-in-the-loop (HIL) system that simulated the impact of mild hybrid electric vehicle (MHEV) operation on the A123 systems 48 V battery pack over U.S. regulatory drive cycles. The HIL system matched charge and discharge data originally generated by Argonne National Laboratory (ANL) during chassis dynamometer testing of a 2013 Chevy Malibu Eco 115 V mild hybrid electric vehicle. All validation testing was performed at the Battery Test Facility (BTF) at the U.S. EPA National Vehicle and Fuel Emissions Laboratory (NVFEL) in Ann Arbor, Michigan. The simulated battery voltages, currents, and state of charge (SOC) of the HIL tests were in good agreement with vehicle test data over a number of different drive cycles and excellent agreement was achieved between RC model simulations of the 48 V battery and HIL battery test data.

### Introduction

The introduction of 48-volt (48 V) mild hybrid electric vehicles (MHEV) has stimulated development of 48 V battery systems capable of providing enhanced driving performance, higher energy density battery packs, and the improved life cycle durability required by consumers and necessary for full-useful-life compliance with U.S. emissions standards. Much of this activity has involved the development of advanced lithium-ion chemistries and in some cases development of variations of deep-cycle lead-acid chemistries such as lead-carbon formulations [1].

Mild hybrid vehicles with 48 V systems have recently appeared in the European light-duty vehicle market due to high fuel prices and stringent new European Union CO<sub>2</sub> passenger car emissions standards. Renault recently introduced the 2017 model year Scenic and Grand Scenic that are 48 V MHEV Diesel multi-purpose-vehicles (MPVs) with a 10 kW electric machine and a 48 V lithium-ion battery originally developed by Continental [2]. The Scenic is approximately eight to ten percent more efficient when using the 48 V MHEV system. Mercedes-Benz introduced a low cost, 12 kW Belt Starter Alternator (BSA, or P0) 48 V MHEV system and

a 15 kW Engine Integrated Starter Alternator (ISA, or P1) 48 V MHEV system with an electrically-driven charge air boosting system for E-class and S-class sedans, respectively [3, 4]. An approximately 20 to 23 percent fuel efficiency was realized via engine downsizing, friction reduction, accessory electrification and 48 V MHEV operation (e.g., torque assist and brake recovery). Audi recently announced introduction of a 48 V MHEV system for the Audi A8 [5].

The Advanced Light-Duty Powertrain and Hybrid Analysis (ALPHA) tool was developed by EPA to model vehicle performance, fuel economy, greenhouse gas (GHG) emissions and battery pack performance for light-duty conventional and hybrid electric vehicles (HEV) [6]. ALPHA can be used as a support tool for future GHG emissions regulations or as a research tool to evaluate the efficiency of new advanced vehicle technologies. The hybrid model within ALPHA is related to EPA's heavy-duty vehicle Greenhouse Gas Emissions Model (GEM) [7] certification tool. Light-duty ALPHA vehicle simulations use the same basic sub-models and controls as heavy-duty vehicle GEM simulations with the exceptions of specific traction motors, generators, batteries, regenerative braking controls, hybrid vehicle supervisory

controls, etc. that differ somewhat between light-duty and heavy-duty applications.

Within MHEV, HEV, and plug-in hybrid electric vehicle (PHEV) applications, an analysis of the battery pack performance, state-of-charge (SOC) trajectory optimization, and optimization of electric motor/internal combustion engine power coupling is of importance since the overall efficiency of the vehicle is closely tied to the efficiency of the battery pack and the energy flows through the hybrid drive system. A two-time constant equivalent circuit battery cell model was developed to closely simulate lithium-ion battery pack voltages. The estimated voltage was then used to calculate traction motor and generator current by dividing it from motor power. The motor power was calculated by multiplying motor torque and motor speed estimated from vehicle supervisory controls. A lumped capacitance battery thermal model was developed to determine battery pack temperature. To rapidly achieve an optimum battery pack temperature of 25 to 40 °C, Battery Management System (BMS) thermal control strategies such as cabin-air heating and variable airflow rates were also implemented within the model.

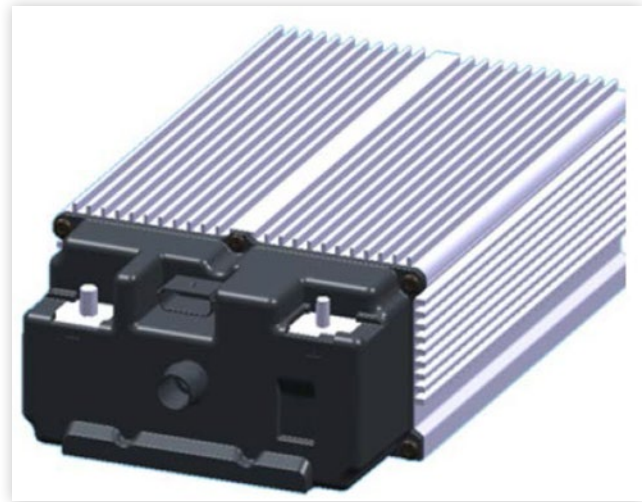
The battery pack model enables fuel economy and GHG emissions to be estimated by simulating the effects of battery cell power capacity, SOC operating window, discharge and charge power limits, battery pack temperatures, battery cell internal resistance, and BMS thermal control strategies.

## Battery Pack Tests

The 0.4 kWh, 48 V, 8 Ah LiFePO<sub>4</sub> battery pack used for testing and simulated during battery modeling was provided by A123 Systems (Livonia, MI USA) (Table 1 and Figure 1). The battery pack was tested at the EPA National Vehicle and Fuel Emissions Laboratory (NVFEL) Battery Test Facility (BTF) to characterize the resistance, capacitance, charge, and discharge behavior of the battery pack.

An AeroVironment AV-900 battery cycler (AeroVironment, Inc., Monrovia, CA USA) was used to provide the demanded power/current to and from the 48 V battery pack for the initial 10 second discharging and charging pulse tests and to follow specific charge/discharge cycles to simulate battery function during vehicle operation. The battery cycler, cooling systems, and control systems used at the NVFEL-BTF allow “hardware-in-the-loop” (HIL) operation that provides a close approximation of battery operating conditions that would exist in-chassis during operation over vehicle regulatory drive cycles such as the Urban Dynamometer

**FIGURE 1** A123 Systems 0.4kWh 8 Ah 48 V Lithium-ion Battery Pack.



US Government / US Environmental Protection Agency

Driving Schedule (UDDS) and the Highway Fuel Economy Test (HwFET) (Figure 2). Input data for HIL operation was based upon chassis dynamometer testing of a 2013 Chevrolet Malibu Eco by Argonne National Laboratory that was conducted as part of the U.S. Department Energy - Vehicle Technologies Office Advanced Vehicle Testing Activity [8, 9, 10]. The Malibu Eco is equipped with a 115 V belt-integrated-starter-generator (BISG or P0) MHEV system. The battery BMS control area network (CAN) communication bus provided battery pack voltages ( $V_{\text{Batt}}$ ) battery pack currents ( $I_L$ ) and battery pack temperatures at 20 Hz/50 ms transmission rates during the tests.

The battery manufacturer provided the Open Circuit Voltage (OCV) curves for the cells, as shown in Figure 3. Power limits were implemented using a two-dimensional look-up table to estimate the effects of SOC and cell/pack temperatures.

As shown in Figure 4, both the charge and discharge power limits are reduced to zero when the battery pack temperature is above 65 °C or below -30 °C, temperatures that represent the upper and lower operating limits for this particular cell chemistry. The desired operating temperature of the battery is between 20 and 55 °C although battery operation can be briefly extended to between -30 and 65 °C. The maximum allowable

**FIGURE 2** Battery Test Setup at EPA NVFEL Battery Test Facility.



US Government / US Environmental Protection Agency

**TABLE 1** 48 V Lithium-Ion Battery Pack Specifications.

Battery Pack Make/Model	A123 Systems, LiFePO <sub>4</sub> “UltraPhosphate”
Battery Pack Serial No.	522702V04C17G1800022
Rated Capacity/Energy	8 Ah/384 Wh
Size (L x W x H)	304 mm x 180 mm x 96 mm
Mass	8 kg
Topology	14S1P

US Government / US Environmental Protection Agency

**FIGURE 3** Open Circuit Voltage ( $V_{OC}$ ) of A123 Systems Lithium-ion Battery Cell at 23 °C.

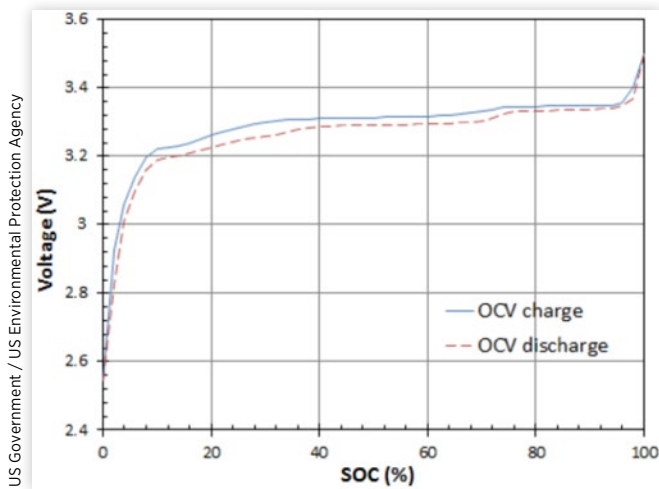
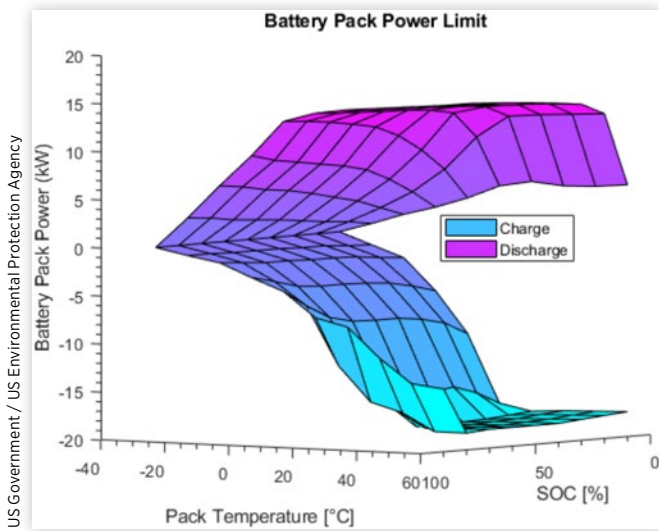


**FIGURE 4** 10 Second Power Limits for the 48 V Lithium-Ion Battery Pack.

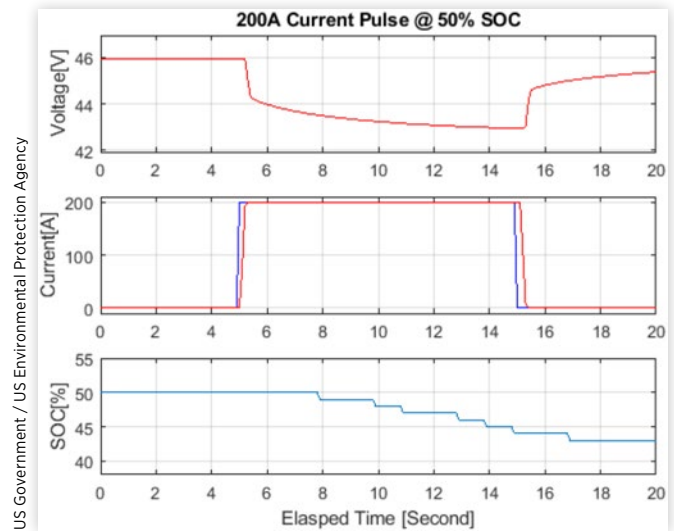


charging and discharging power limits of the 48 V battery pack are 16 kW and 15 kW, respectively, at 50% SOC and a 25 °C battery pack temperature near the beginning-of-life. The BMS has a self-balancing SOC control function. At -30 °C, the battery can still discharge at approximately 30 A for 10 seconds at 50% SOC, which is sufficient to crank the engine for cold starts. The 10 second discharging and charging current limits are approximately 370 A between 30% SOC and 60% SOC and for pack temperatures between 30 and 60 °C.

Figure 5 shows that the demanded current (blue line) from the AV900 battery cyler has an approximately 100~200 ms delay in order to reach the requested current (red line). The battery pulse currents achieved were offset from the demanded current due to CAN-based data transmission rates that are limited to 10 Hz/100 ms.

The ohmic short/long-time resistances and capacitances are calculated by using 10 second current pulse test data. As shown in Figure 6, the time constant ( $\tau$ ) for the short-time

**FIGURE 5** 200 A 10 Second Discharging Pulse Test.



resistances and capacitances was calculated by taking the time from the start of the pulse test to the point where the blue-colored curve intersects with a 45° line from the horizontal (shown by the dashed red line). The short-time-interval capacitance and resistance ( $R_{ST}$  and  $C_{ST}$ , respectively) and long-time-interval capacitance and resistance ( $R_{LT}$  and  $C_{LT}$ , respectively) can be calculated by estimating cell voltage recovery response gradients [11] when running high I-V (current-voltage) discharging and charging current pulse tests at various SOC levels. However, voltage response gradients from battery pack I-V tests may be different from the voltage response gradients of battery cell I-V tests due to cell-to-cell SOC imbalance, cell-to-cell voltage variations, etc.

As shown in Figure 7, the measured battery pack ohmic short/long time resistances and capacitances are significantly reduced compared to those of typical lithium-ion battery packs to maintain the battery pack voltages within the desired voltage range between 36 V and 52 V even during very high

**FIGURE 6** A Time Constant ( $\tau$ ) for the short-time resistance and Capacitance.

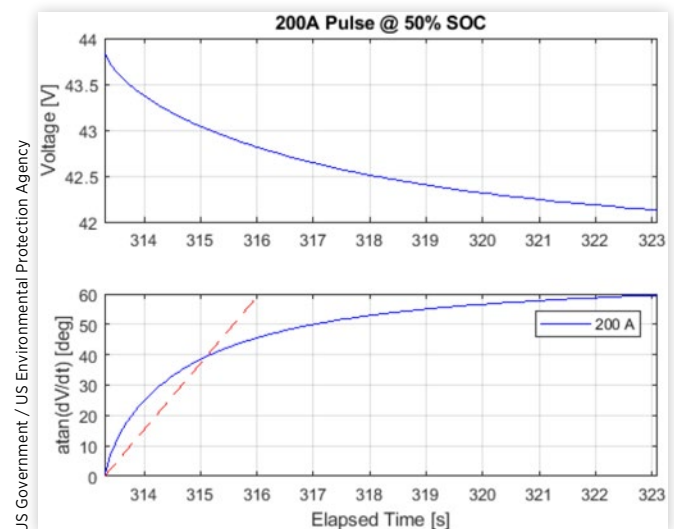
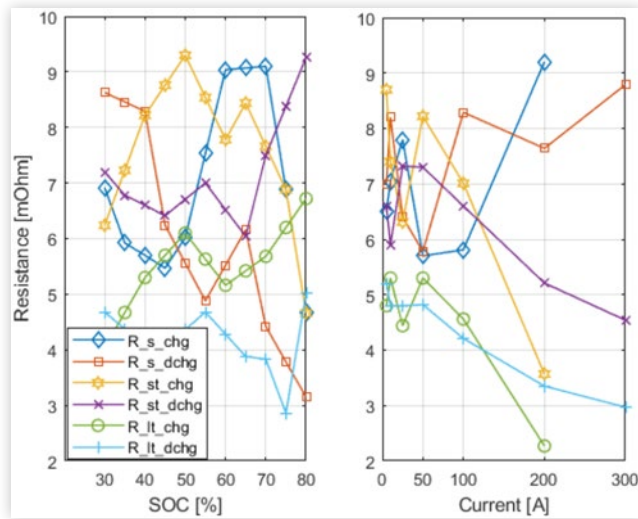




**FIGURE 7** Ohmic Resistances of 48 V 14 Cell Lithium-Ion Battery Pack.

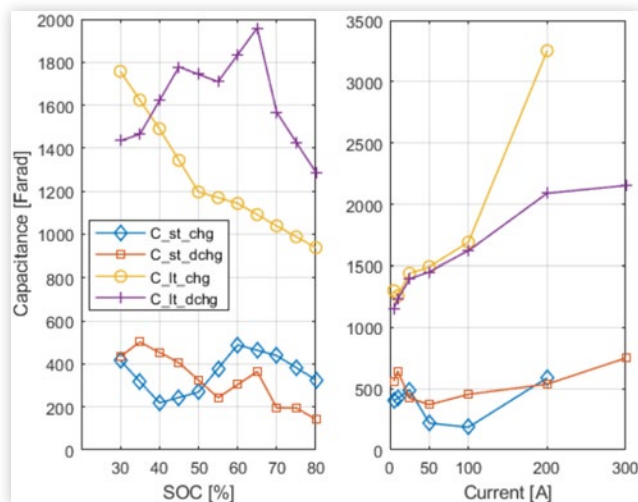


current discharging and charging events. The measured 8 to 10 milliohm ( $m\Omega$ ) ohmic resistances of this pack are low, suggesting optimization for 48 V MHEV applications. The measured ohmic short and long duration resistances for the pack were implemented within MATLAB/Simulink lookup tables to estimate the effects of SOC and 10 second charging/discharging current pulse tests.

Ohmic resistances during charging ( $R_{s\_chg}$ ) are higher than the ohmic resistances during discharging ( $R_{s\_dchg}$ ), as shown in Figure 7. Similarly, RC short time constants during charging ( $\tau_{st\_chg}$ ) are higher than those of discharging ( $\tau_{st\_dchg}$ ), as shown in Figure 8.

In automotive 48 V MHEV applications, the lower nominal voltage 48 V battery pack experiences higher discharging and charging current than previous higher voltage MHEV pack designs, such as the original Malibu Eco 115 V MHEV, when delivering or receiving the same electric power to and from the vehicle.

**FIGURE 8** Capacitances of 48 V 14 Cell Lithium-Ion Battery Pack.



## Battery Pack Model

The Battery Pack Model in ALPHA consists of an equivalent circuit cell model, a battery thermal model, and BMS controls. Accurate SOC, discharge power, and charge power limits are required to estimate available traction motor power and torque precisely.

### Equivalent Circuit Cell Model

A two-time constant equivalent circuit model [12, 13, 14] was applied to calculate terminal voltages for a lithium-ion polymer cell. Battery pack voltages were calculated by multiplying by the number of cells in series within the battery pack.

In Figure 9, the  $V_{oc}$  is the open circuit voltage of a cell.  $R_o$  is the ohmic resistance of a cell, and is dependent on the SOC and cell/pack temperatures.  $R_{ST}$  and  $C_{ST}$  are resistances and capacitances of the electro-magnetic short-time-interval double layer effects, respectively.  $R_{LT}$  and  $C_{LT}$  are resistances and capacitances of the electro-chemical long-time-interval mass transport effects, respectively.  $I_L$  is the cell load current. Discharge current is positive while negative current represents charging.

Battery cell terminal voltage,  $V_L$ , can be calculated by using a typical RC circuit equation (1).

$$V_L = V_{OC} + I_L * R_o + \int (I_L - I_{ST})/C_{ST} dt + \int (I_L - I_{LT})/C_{LT} dt \quad (1)$$

$$\text{where } I_{ST} = V_{ST}/R_{ST} \text{ and } I_{LT} = V_{LT}/R_{LT}.$$

Battery pack voltage,  $V_{Batt}$ , was calculated using equation (2):

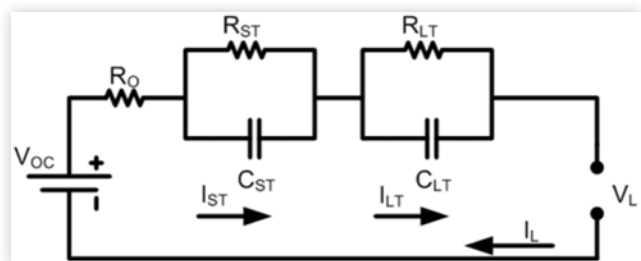
$$V_{Batt} = V_L * N_{series} / N_{parallel} \quad (2)$$

where  $N_{series}$  is 14 cells with series connections and  $N_{parallel}$  is one parallel connection for this particular 48 V pack. Battery pack voltages,  $V_{Batt}$ , and battery pack currents,  $I_L$ , were obtained from the vehicle CAN communication bus during vehicle chassis-dynamometer testing.

### Battery Thermal Model

The lumped capacitance battery thermal model [14, 15, 16] in ALPHA was developed to feed battery pack temperature information to a battery voltage control block, battery power limit control block, and BMS control strategies.

**FIGURE 9** Battery Equivalent Circuit Cell Model.



The battery pack temperature was calculated in [equation \(7\)](#) by using the energy balance between battery heat generation,  $Q_{ees\_gen}$ , and heat loss,  $Q_{ees\_cooling}$ , while also considering the thermal mass of the battery pack and the method of cooling:

$$T_{ees} = \int_0^t \frac{(Q_{ees\_gen} - Q_{ees\_cooling})}{m_{ees} C_{p,ees}} dt + T_0 \quad (7)$$

where  $m_{ees}$  is the mass of the battery pack electric energy storage system,  $T_0$  is the initial pack temperature, and  $C_{p,ees}$  is battery heat capacity [[15](#), [16](#), [17](#), [18](#)].

The  $Q_{ees\_gen}$  is calculated by [equation \(8\)](#):

$$Q_{ees\_gen} = I_L^* R_{Batt}^2 + (1 - \text{charge efficiency})^* I_L^* V_{Batt} \quad (8)$$

The battery pack resistance,  $R_{Batt}$ , is obtained using [equation \(9\)](#):

$$R_{Batt} = (R_O + R_{ST}^* I_{ST} / I_L + R_{LT}^* I_{LT} / I_L) * N_{series} / N_{parall} \quad (9)$$

where  $R_O$  is battery cell discharging, or charging resistance. The cell resistance,  $R_O$ , is estimated by using a 2-dimensional discharge look-up table when battery current is positive, and by using the charging resistance when battery current is negative.

The  $Q_{ees\_cooling}$ , is calculated by using [equation \(10\)](#):

$$Q_{ees\_cooling} = (h A_s + kt)(T_{ees} - T_{coolant}) \quad (10)$$

where  $T_{coolant}$  is the battery pack inlet coolant temperature which, depending on pack configuration, can be the temperature of the ambient air, the cabin-conditioned air, or the liquid water coolant depending on the battery cooling system design.  $A_s$  is the battery surface area for convection heat transfer and  $t$  is the thickness of the battery pack for heat transfer via conduction. A typical battery conduction coefficient,  $k$ , and convection coefficient,  $h$ , were found in published references [[15](#), [16](#), [17](#)]. The lumped thermal equations were implemented by using MATLAB/Simulink blocks. The specifications from [Table 1](#) and [Figure 10](#) were used to validate the battery model within ALPHA.

## Battery Management System Controls

Battery cooling control strategies were also implemented to emulate typical HEV BMS cooling controls. With sufficient cooling, the pack temperature can be decreased to the cooling OFF temperature, and the cooling ON strategy can be reactivated after the pack temperature rises to the specified cooling ON temperature. The cooling ON/OFF temperature settings can be calibrated for typical vehicle operating conditions such as operation in regions with hot and cold temperatures. There is no active battery cooling when the pack temperature is below 25 °C, and an active battery heating system may be required when the pack temperature is extremely low under cold ambient conditions. The tested A123 Systems 48 V battery pack was not equipped with active cooling. Instead, it uses

passive air cooling with aluminum fins and has a vent for expelling battery gases in the event of a cell failure. Hence, passive air cooling was used during model validation.

The available Discharge Power Limit (DPL), was calculated using [equation \(11\)](#):

$$DPL_{avail} = DPL(\overline{SOC}(t)) - DPL(\overline{minimum SOC}) \quad (11)$$

where  $DPL_{avail}$  is the available discharge power limit,  $DPL(SOC)$  is the discharge power limit at a given SOC, and the minimum SOC is 30%. The typical SOC maximum in MHEVs is 80%, and the maximum, high, low, and minimum values of the SOC windows can be calibrated to optimize battery cell performance and cell durability for MHEV vehicle applications. The battery pack can provide sufficient electric power to a P0 (e.g., BISG) or inline P2 (e.g., clutched/transmission-integrated) traction motor when the required road load power is less than the available discharge power limit. The available discharge power is used to turn on the internal combustion engine if the demanded road-load power is greater than the available discharge power. The battery discharge power limits vary depending on pack temperature and SOC level.

For final SOC balancing, the following Proportional-Integral-Derivative (PID) controller algorithm was employed during model simulation:

$$\Delta Power_{Batt} = PL(\overline{SOC}(t)) - PL(\overline{SOC}_{target})$$

$$Power_{comp} = \Delta Power_{Batt} + k_p \Delta SOC(t) + k_i \int \Delta SOC(t) dt + k_d \frac{d}{dt} \Delta SOC(t) dt \quad (13)$$

$$\Delta SOC(t) = SOC(t) - SOC_{target}, k_p = 15.7, k_i = 3.5, k_d = 0.018$$

where Power Limit,  $PL$ , is the discharge and charge power limit for positive current, and for negative current respectively.

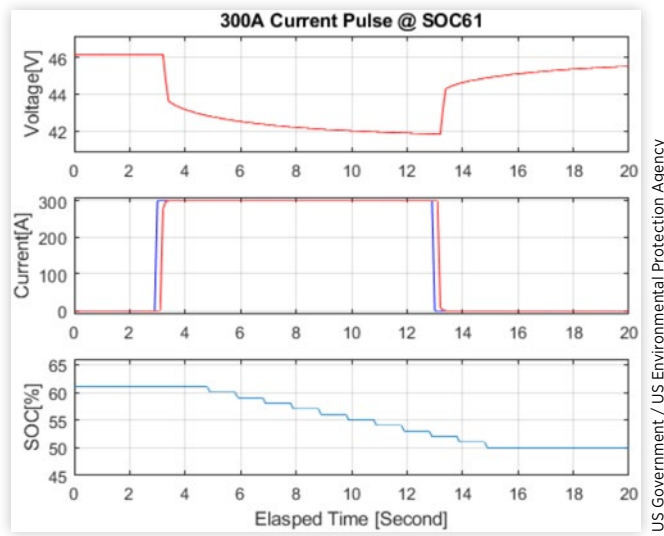
## Battery Model Validation

[Figure 10](#) shows that the pack can maintain the desired battery voltage levels between 36 V and 52 V under 300 A high current pulse tests although the battery pack SOC was reduced by approximately 10% during the 10-second pulse test.

As shown in [Figure 11](#), the simulated discharging and charging battery pack voltages are in good agreement with the 48 V battery test data. The root-mean-squared (RMS) voltage differences between the simulated discharging and charging pack voltage and the RMS voltage differences of the test data are within 0.11 V during a 200 A 10-second pulse test. The simulated voltage was quickly recovered by completing the discharging pulse current inputs and the pack voltage during the 48 V lithium-ion battery pack tests returned slowly to the open circuit voltage.

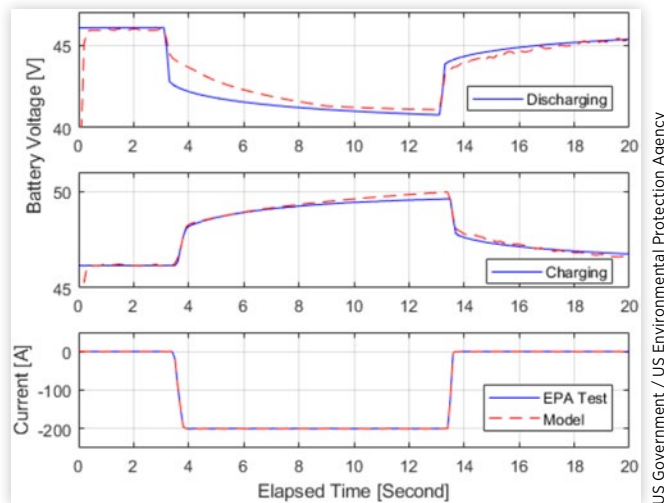
Modeled and HIL-measured battery pack RMS voltage, power, SOC and temperature over the UDDS cycle are compared in [Figure 12](#). The RMS voltage differences between the simulated voltages and the HIL test data shown were approximately 0.8 V RMS, and the simulated voltage averages were within 0.7% of the HIL test data averages over the UDDS driving cycle ([Figure 12A](#)).

**FIGURE 10** A 300 Ampere Discharging Current Pulse Test at 60% SOC.



US Government / US Environmental Protection Agency

**FIGURE 11** Discharging/Charging Pulse Tests at 50% SOC.

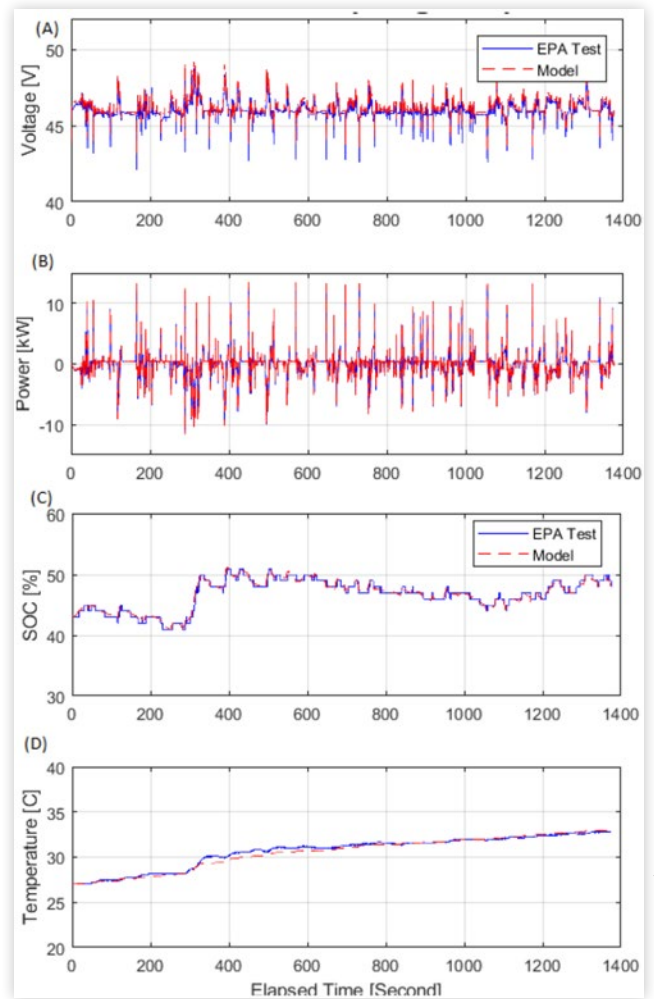


US Government / US Environmental Protection Agency

The modeled 48 V battery pack power and SOC were in good agreement with the HIL test data (Figure 12B and C). The captured RMS regenerative braking energy differences between the modeled 48 V battery pack and those of the HIL battery test data were within 0.12 kW. Modeled battery pack temperatures (Figure 12D) were also in excellent agreement with HIL battery test data. The modeled 46.2 V RMS and the measured 46.01 V RMS battery pack voltages over the HIL simulation of the UDDS cycle were in good agreement. The modeled 30.58 °C RMS temperatures and the measured 30.71 °C RMS pack temperatures were also in an excellent agreement, and the pack temperature was increased about 6 °C over the HIL UDDS simulation test when using the 2013 Malibu Eco chassis dynamometer test battery charge/discharge power profiles. The battery pack can maintain the desired voltage levels between 36 and 52 V at a current of 47.2 A RMS during the UDDS driving cycle.

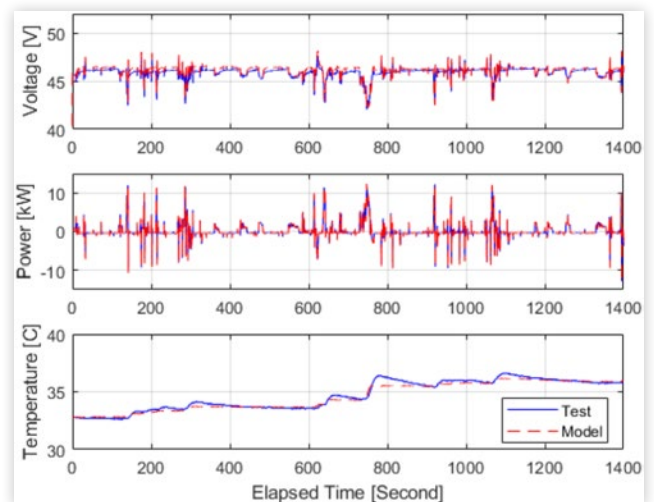
As shown in the first plot in Figure 13, the battery pack can also hold the desired operating voltage levels between 36

**FIGURE 12** Modeled (red) and Measured (blue) Power (A), Voltage (B), SOC (C), Battery Temperature (D) for a 48 V Lithium-Ion Battery Pack during HIL Simulation of the UDDS Cycle.



US Government / US Environmental Protection Agency

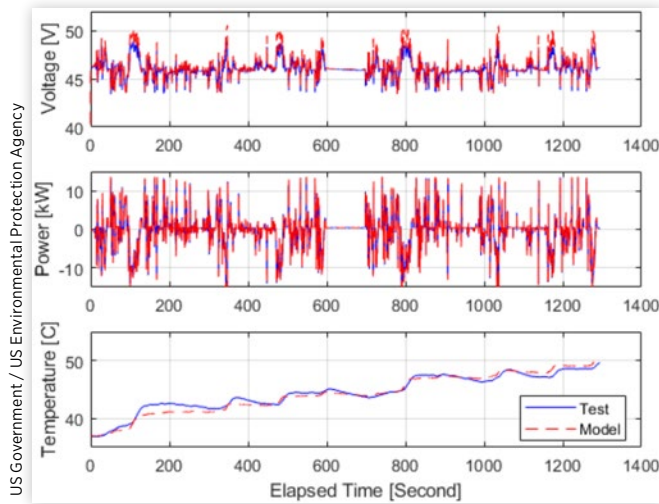
**FIGURE 13** Modeled (red) and Measured (blue) Voltages and Temperatures for the 48 V Battery during HIL Simulation of the HwFET Cycle.



US Government / US Environmental Protection Agency



**FIGURE 14** Modeled (red) and Measured (blue) Voltages and Temperatures for the 48 V Battery during HIL Simulation of the US06 cycle.



and 52 V at a current of 48.1 A RMS during the HwFET driving cycle. The modeled 46.03 V and 48.1 A RMS pack voltage and current and the 45.87 V and 48.1 A RMS pack voltages and current measured during HIL battery testing over the HwFET were in good agreement.

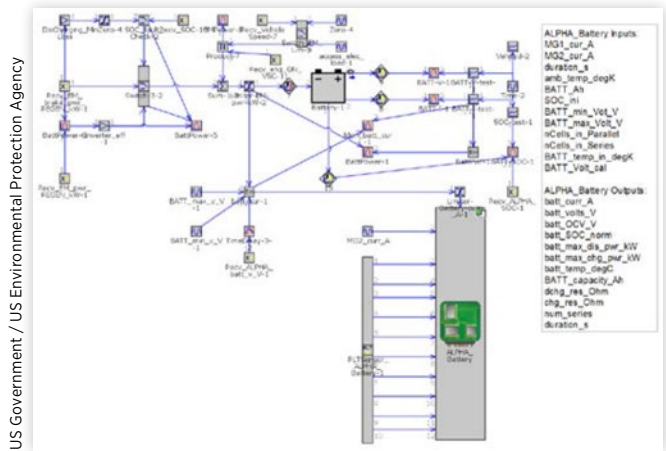
A 795 J/kg-K specific heat capacity [15, 16] and 18.9 W/m<sup>2</sup>-K heat transfer coefficient [17] for the battery pack and a 0.25 W/m-K heat conductivity for the case material served as inputs into the thermal model. The temperature surrounding the battery pack was assumed to be approximately 30 °C at the BTF when calculating heat conduction from or to the battery pack. The modeled 34.81 °C RMS temperatures and the measured 34.95 °C RMS pack temperatures were in excellent agreement. As shown in Figure 13, the battery temperature from the test data and model simulations are in good agreement.

As shown in the first plot in the Figure 14, the battery pack can still hold the desired operating voltage levels between 36 and 52 V at a current of 88.2 A RMS during operation over the higher speeds, loads, and accelerations represented in the US06 driving cycle [19]. The modeled 46.19 V and 88.2 A RMS voltage and current and the HIL-measured 46.04 V and 88.2 A RMS voltage and current are in good agreement. The modeled 44.36 °C RMS pack temperatures and the measured 44.56 °C RMS pack temperatures were in an excellent agreement. The pack temperature was increased approximately 12.7 °C from the initial 37 °C pack temperature during HIL testing when using charge/discharge data from chassis dynamometer testing of the 2013 Malibu Eco over the US06 cycle. Even assuming passive cooling, the pack was able to maintain pack temperatures within an acceptable operating range for operation over two back-to-back US06 drive cycles.

## Battery and Vehicle Model Co-Simulations

As shown in Figure 15, the Gamma Technology GT-DRIVE vehicle model was used to simulate 48 V MHEV models at an early conceptual stage [20]. The EPA’s engine and battery

**FIGURE 15** Schematic of the GT-Suite Battery and ALPHA Battery Model DLL (A larger version is reproduced within the Appendix for purposes of readability).

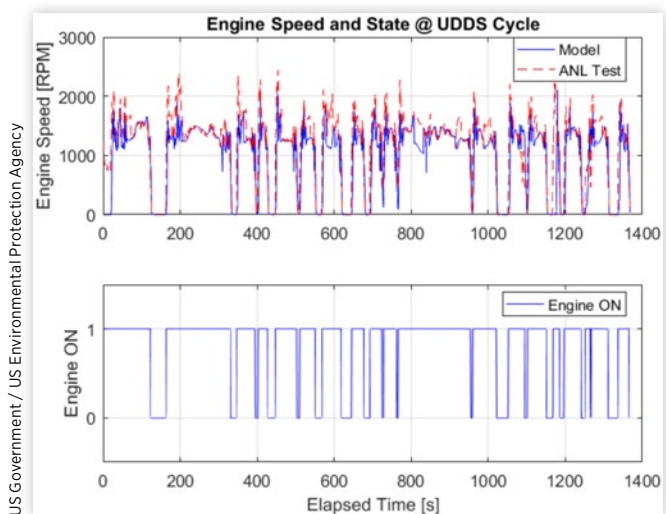


models were compiled using Microsoft Visual Studio 10 and the 2016a version of the MATLAB/Simulink/Stateflow toolbox to create a dynamic link library (DLL). The ALPHA battery DLL was critical to calculate battery discharge and charge power limits, battery charging efficiency, pack temperature, etc., precisely during vehicle drive cycle simulations. A smart utilization of battery power is of paramount importance for any vehicle electrification application and for proper modeling of vehicle GHG emissions and fuel consumption.

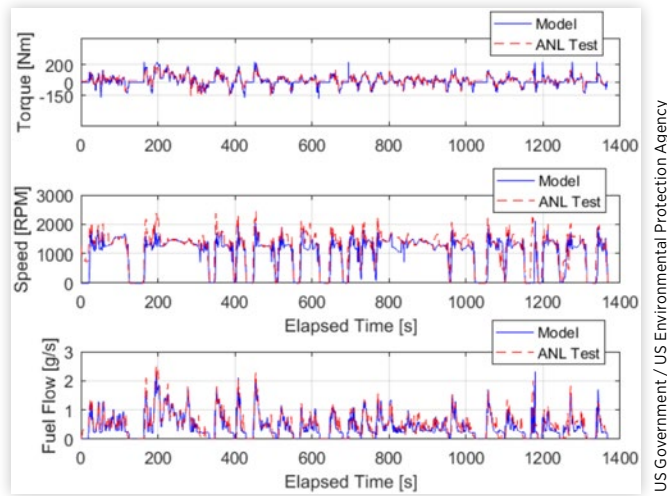
A DLL was developed to simulate the A123 Systems lithium-ion battery cell used within the 48 V MHEV battery pack, and the DLL was used to build a GT-DRIVE simulation of a 48 V BISG (P0) MHEV version of the 2013 Chevrolet Malibu Eco [20]. This vehicle was originally equipped with a higher voltage, 0.5 kWh 4.4 Ah 32 cell 115 V lithium-ion battery pack and 12/15 kW (charge/discharge) BISG MHEV system.

Figure 16 shows that the 1071 seconds of engine-on time from the 48 V MHEV model simulation was in excellent

**FIGURE 16** Engine Speed and Engine state of 2013 GM Malibu Eco over the UDDS.



**FIGURE 17** Modeled 48 V MHEV (Blue) and Measured 115 V MHEV Engine Torque & Fuel Flow over the UDDS.



US Government / US Environmental Protection Agency

agreement with the 1070 seconds of engine-on time from the ANL 115 V MHEV test data over the UDDS [9, 10]. Therefore, the simulated engine-on time and the engine-on time of the test data were comparable when using the available discharge battery power limits.

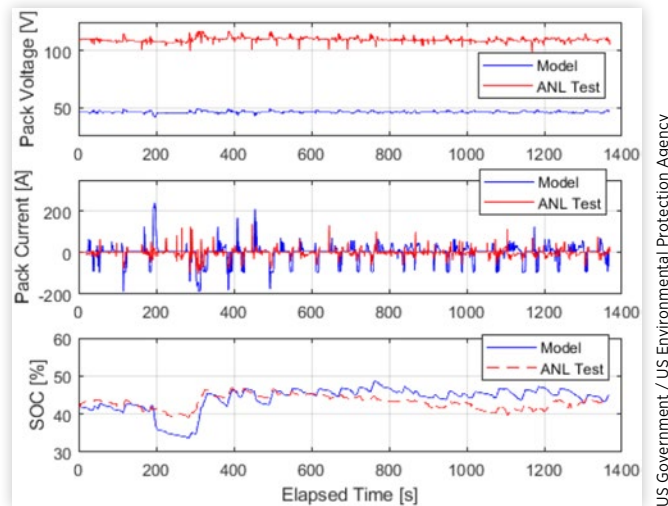
As shown in Figure 17, the simulated engine torque for the 48 V MHEV operated within a region of higher engine efficiency to minimize fuel consumption, similar to the 115 V MHEV test data. The trends of engine torque and speed for the GT- DRIVE 48 V MHEV simulation were in good agreement with those of the Malibu Eco 115 V MHEV chassis dynamometer test data [9, 10]. The 57.1 Nm RMS engine torque for the simulated 48 V MHEV was within 4.5% of the 54.7 N-m RMS engine torque 115 V MHEV test data [21, 22]. Overall, the simulated engine torque and speed shown in Figure 17 were in good agreement with the simulated engine torque and speed of the chassis dynamometer test data generated by ANL.

The estimated motor current and accessory current were used as inputs into the battery pack model to estimate the battery pack SOC and voltage. Charge efficiencies and battery pack temperature were also considered when estimating the battery pack SOC.

As shown in Figure 18, the 42.7A RMS current for the 48 V MHEV was significantly higher when compared to the 17.9 A RMS current for the 115 V MHEV test data over the UDDS [9, 10] due to the battery pack voltage change from 115 V to 48 V. The simulated final SOC of the 48 V battery pack had lower discharged battery power and higher final SOC than what was found during the ANL UDDS tests of the 115 V MHEV version of the vehicle, and thus represent conservative estimations with respect to GHG emissions. The SOC swing windows of the modeled 0.4kWh 48 V battery pack are greater than the SOC windows of the original equipment manufacturer (OEM) 0.5kWh 2013 Malibu Eco 115 V battery pack since the SOC varies more quickly due to the reduced storage capacity of the 48 V pack when charging and discharging the same electric power as the higher capacity and higher voltage OEM battery pack.

The simulation shows that similar UDDS and HwFET cycle fuel economy and GHG emissions can be achieved (Table 3) by

**FIGURE 18** Modeled 48 V MHEV (Blue) and Measured 115 V MHEV Battery Pack Voltage, Current, and SOC over the UDDS.



US Government / US Environmental Protection Agency

**TABLE 3** UDDS and HwFET Cycle Fuel Economy of 48/115 V MHEVs.

Driving Cycle	Initial / Final SOC (%)	CO <sub>2</sub> (g/km)	Fuel Economy (mpg)	Remark
115 V UDDS /w 0.5 kWh	42/43.3	162.4	34.0	ANL Test [9, 10]
	42/44.6	161.0	34.3	Model
48 V UDDS /w 0.4 kWh	42/45.1	161.9	34.1	Model
115 V HwFET /w 0.5 kWh	43/48.3	112.9	48.9	ANL Test [9, 10]
	43/43.1	113.6	48.6	Model
48 V HwFET /w 0.4 kWh	43/46.7	115.3	47.9	Model

US Government / US Environmental Protection Agency

using a 0.4 kWh, 48 V battery pack and MHEV system in place of the OEM 0.5 kWh 115 V battery pack and system, with the potential for significantly reducing battery pack weight and size. Additional weight reduction could be realized by using an inverter-integrated 48 V electric machine and eliminating the long three-wire, three-phase AC cables from the rear trunk area of the Malibu Eco to the BISG motor near the engine pulley location. The simulation did not consider the weight-savings from the smaller, lighter 48 V lithium ion pack or from inverter integration into the electric machine.

The battery pack power-limit-based engine ON/OFF control strategy enabled fuel economy and GHG emissions to be estimated with improved precision by updating battery cell capacity, the minimum SOC set points, etc., during drive-cycle modeling runs. Increased fuel economy and GHG emission reduction could also be achieved by improving battery cell power limits without changing the minimum SOC set points. This control strategy would be useful to optimize the best SOC operating window range when increasing battery cell power output via battery cell chemistry improvements, thermal management improvements, or other system design changes.



## Summary and Conclusions

A two-time constant equivalent circuit battery cell model along with a lumped capacitance thermal model and BMS control strategies were implemented within a model of a 48 V MHEV battery pack, for incorporation into the EPA ALPHA model and Gamma Technology GT- DRIVE vehicle simulations to explore various combinations of advanced future HEV technologies. Excellent agreement between battery model simulations and test data was achieved. In addition, model simulation time was significantly reduced by using simple and computationally efficient models.

The electric circuit battery model was incorporated as a DLL into a 48 V MHEV model for vehicle level drive-cycle co-simulation using the Gamma Technology GT-DRIVE model. This model was used to simulate GHG emissions and fuel economy of a BISG 48 V MHEV with a second-by-second time resolution. Vehicle models such as GT-DRIVE and the EPA ALPHA model can be used to quantify the effectiveness of new advanced vehicle technologies by estimating the relative improvement in GHG emissions, fuel economy, and vehicle and battery pack performance.

The look-up table based OCV, internal resistances and discharge/charge power limits within the battery pack model can be easily updated as new lithium-ion cell chemistries are developed for hybrid electric vehicles or battery electric vehicles. The data-driven battery pack model and mathematical-rule-based vehicle supervisory controls in the ALPHA and GT-DRIVE co-simulation vehicle models enable fuel economy and GHG emissions to be estimated by optimizing various battery pack design variables, SOC operating windows, BMS cooling strategies, battery pack power, and pack energy capacity.

Co-simulations of GT-DRIVE and the ALPHA vehicle model can be used to optimize lithium-ion battery pack design parameters to meet vehicle electrification power demand by implementing a two-time constant equivalent circuit battery cell model, a lumped battery thermal model and typical MHEV VSC and BMS control strategies. The 48 V lithium-ion battery pack model was validated with HIL battery test data generated at the EPA NVFEL battery test laboratory in Ann Arbor and using 2013 Chevrolet Malibu Eco chassis dynamometer test data generated by ANL.

## References

- Kelly, J., Scanes, P., and Bloore, P., "Specification and Design of a Switched Reluctance 48 V Belt Integrated Starter Generator (B-ISG) for Mild Hybrid Passenger Car Applications," SAE Technical Paper [2014-01-1890](#), 2014, doi:[10.4271/2014-01-1890](#).
- Pothin R. and Dolcini P., "Deployment of 48 V in Renault, Current Status and Future Outlook," Proceedings -Internationaler Motorenkongress 2017, Springer Vieweg, Wiesbaden.
- Kemmler, R., Kreitmann, F., Werver, M., and Inderka, R., "M 264 - The New Mercedes-Benz 4-Cylinder Toptype-Gasoline Engine with 48 V-Electrification." *38<sup>th</sup> International Vienna Motor Symposium*, 2017.
- Vollrath, O., Banken, J., Lautenschütz, P., and Storz, O., "M 256 - the New Mercedes-Benz High-Performance Six-Cylinder In-Line Gasoline Engine with Intelligent 48 V Electrification," *38<sup>th</sup> International Vienna Motor Symposium*, 2017.
- Jablonski C., Schimmel C., and Underberg V., "The Chassis of the All-new AUDI A8," Proceedings - *8<sup>th</sup> International Munich Chassis Symposium*, 2017, Springer Vieweg, Wiesbaden.
- Lee, B., Lee, S., Cherry, J., Neam, A. et al., "Development of Advanced Light-Duty Powertrain and Hybrid Analysis Tool (ALPHA)," SAE Technical Paper [2013-01-0808](#), 2013, doi:[10.4271/2013-01-0808](#).
- Lee, S., Lee, B., Zhang, H., Sze, C. et al., "Development of Greenhouse Gas Emissions Model for 2014-2017 Heavy- and Medium-Duty Vehicle Compliance," SAE Technical Paper [2011-01-2188](#), 2011, doi:[10.4271/2011-01-2188](#).
- U.S. Department of Energy - Office of Energy Efficiency and Renewable Energy - Vehicle Technology Office. "Advanced Vehicle Testing Activity Data and Results," <https://energy.gov/eere/vehicles/advanced-vehicle-testing-activity-avta-data-and-results>, Dec. 2017.
- U.S. Department of Energy - Office of Energy Efficiency and Renewable Energy - Vehicle Technology Office. "AVTA: 2013 Chevrolet Malibu HEV Testing Results," <https://energy.gov/eere/vehicles/downloads/avta-2013-chevrolet-malibu-hev-testing-results>, Dec. 2017.
- Argonne National Laboratory. "2013 Chevrolet Malibu Eco" from the Downloadable Dynamometer Database, <http://www.anl.gov/energy-systems/group/downloadable-dynamometer-database/hybrid-electric-vehicles/2013-chevrolet>, Dec. 2017.
- Schweighofer, B., Raab, K.M., and Brasseur, G., "Modeling of High Power Automotive Batteries by the Use of an Automated Test System," *IEEE Transaction on Instrumentation and Measurement* 52(4):1087-1091, 2003, doi:[10.1109/TIM.2003.814827](#).
- Chen, M. and Rincon-Mora, G.A., "Accurate Electrical Battery Model Capable of Predicting Runtime and I-V Performance," *IEEE Transaction on Energy Conversion* 21(2):504-511, 2006, doi:[10.1109/TEC.2006.874229](#).
- Lee, S., Lee, B., McDonald, J., and Nam, E., "Modeling and Validation of Lithium-ion Automotive Battery Packs," SAE Technical Paper [2013-01-1539](#), 2013, doi:[10.4271/2013-01-1539](#).
- Lee, S., Lee, B., McDonald, J., and Safoutin, M., "HIL Development and Validation of Lithium-Ion Battery Packs," SAE Technical Paper [2014-01-1863](#), 2013, doi:[10.4271/2014-01-1863](#).
- Pesaran, A.A., "Battery Thermal Models for Hybrid Vehicle Simulations," *Journal of Power Sources* 110(2):377-382, 2002, doi:[10.1016/50378-7753\(02\)00200-8](#).
- Pesaran, A.A. and Keyser, M., "Thermal Characteristics of Selected EV and HEV Batteries," Annual Battery Conference: Advances and Applications, Long Beach, California, Jan. 2001.
- Ismail, N., Toha, S., Azubir, N., Izhak, N. et al., "Simplified Heat Generation Model for Lithium Ion Battery Used in Electric Vehicle," *IOP Conference Series: Materials Science and Engineering* 53:012014, 2013, doi:[10.1088/1757-899X/53/1/012014](#).

18. Catherino, H.A., "Estimation of the Heat Generation Rates in Electrochemical Cells," *Journal of Power Sources* 239(1):505-512, 2013, doi:[doi.org/10.1016/j.jpowsour.2013.03.169](https://doi.org/10.1016/j.jpowsour.2013.03.169).
19. U.S. Code of Federal Regulations, Title 40, Part 86, § 86.158-00, 2000.
20. Lee, S., Cherry, J., Safoutin, M., McDonald, J. et al., "Modeling and Controls Development of 48 V Mild Hybrid Electric Vehicles," SAE Technical Paper [2018-01-0413](https://doi.org/10.4271/2018-01-0413), 2018, doi:[10.4271/2018-01-0413](https://doi.org/10.4271/2018-01-0413).
21. Rask, E., Duoba, M., Lohse-Busch, H., and Walsh, P., "Advanced Technology Vehicle Lab Benchmarking - Level 2 (in-depth)," presentation at the 2012 U.S. Department of Energy Hydrogen Program and Vehicle Technologies Annual Merit Review.
22. Lohse-Busch, H., "Advanced Technology Vehicle Lab Benchmarking - Level 1," presentation at the 2013 U.S. Department of Energy Hydrogen Program and Vehicle Technologies Annual Merit Review.

## Contact In formation

### SoDuk Lee, Ph.D.

Assessment & Standards Division  
 US EPA - Office of Transportation & Air Quality  
 2000 Traverwood Drive, Ann Arbor, MI 48105  
 734-214-4373  
[lee.soduk@epa.gov](mailto:lee.soduk@epa.gov)

## Disclaimer

This document has been reviewed in accordance with U.S. Environmental Protection Agency policy and approved for publication. The views expressed by individual authors, however, are their own, and do not necessarily reflect those of the U.S. Environmental Protection Agency.

## Acknowledgments

The authors would like to acknowledge the following persons for their cooperation to this model development and validation:

- Eric Rask, Michael J. Duoba, Kevin Stutenberg and Henning Lohse-Busch at Argonne National Laboratory for sharing chassis dynamometer test data.

- Tim Burress at Oak Ridge National Laboratory for providing electric motor efficiency test data.
- Mr. Joseph Wimmer and Ryan Tooley at Gamma Technologies for their extensive technical support with GT-DRIVE.

## Definitions/Abbreviations

**ALPHA** - Advanced Light-Duty Powertrain and Hybrid Analysis

**ANL** - Argonne National Laboratory

**BSA** - Belt starter-alternator

**BTF** - Battery test facility

**BISG** - Belt integrated starter generator

**BMS** - Battery management system

**DLL** - Dynamic link library

**DPL** - Discharge power limit

**EPA** - U.S. Environmental Protection Agency

**GEM** - Greenhouse Gas Emissions Model

**GHG** - Greenhouse gas

**HEV** - Hybrid electric vehicle

**HIL** - Hardware-in-the-loop

**HwFET** - Highway fuel economy test procedure

**ISA** - Integrated starter-alternator

**LD** - Light duty

**MHEV** - Mild hybrid electric vehicle

**MPV** - Multi-purpose vehicle

**NVFEL** - National Vehicle and Fuel Emissions Laboratory

**OCV** - Open circuit voltage

**OEM** - Original equipment manufacturer

**PHEV** - Plug-in hybrid electric vehicle

**PID** - Proportional-integral-derivative

**RC** - Resistance-capacitance

**RMS** - Root mean square

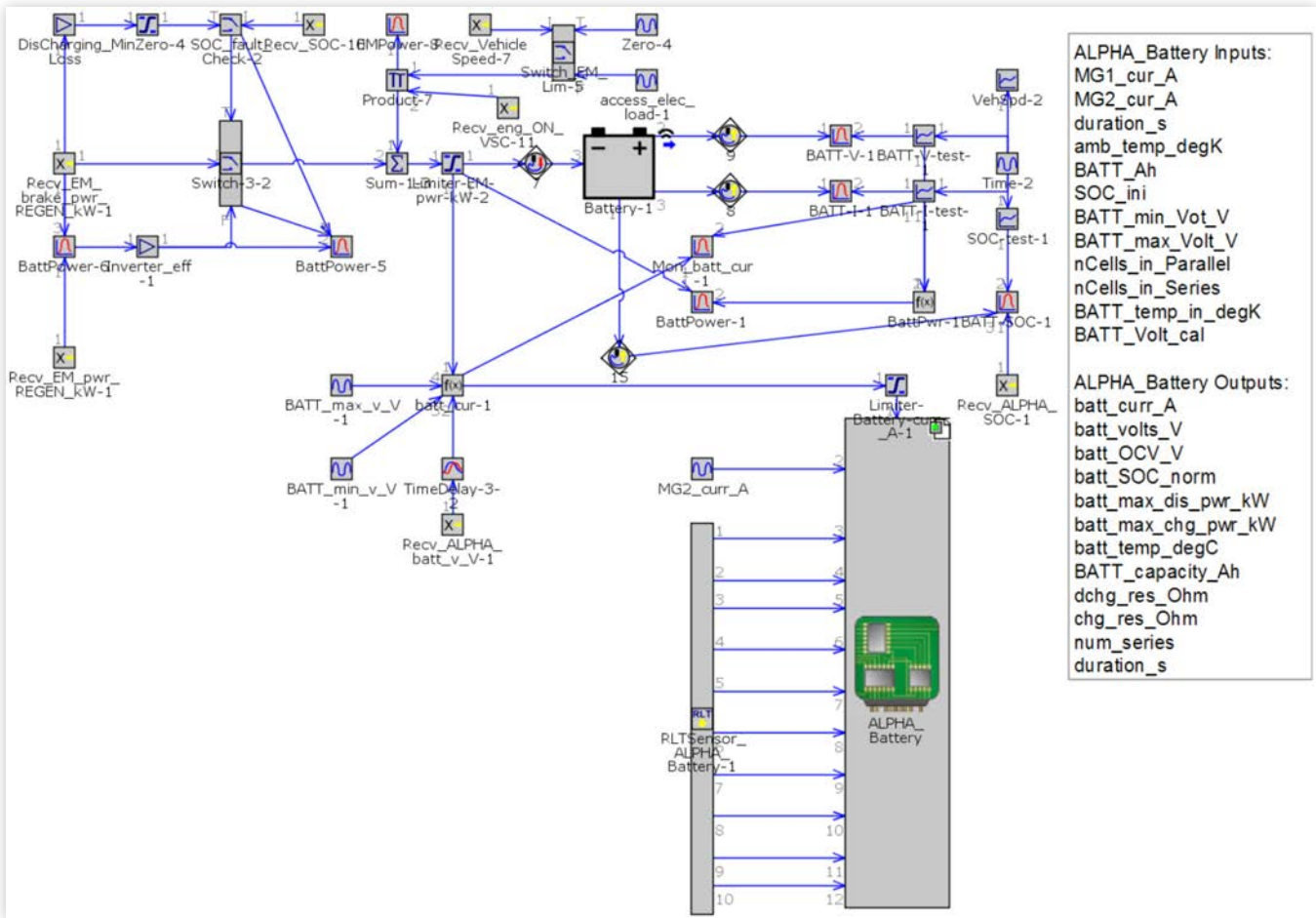
**SOC** - State of charge

**UDDS** - Urban dynamometer driving schedule

**VSC** - Vehicle supervisory control

# Appendix

**APPENDIX FIGURE 1** Schematic of the GT-Suite Battery and ALPHA Battery Model DLL.



US Government / US Environmental Protection Agency

This is a declared work of the U.S. Government and is not subject to U.S. copyright protection. Foreign copyrights may apply. The U.S. Government assumes no liability or responsibility for the contents of this paper or the use of this paper, nor is it endorsing any manufacturers, products, or services cited herein and any trade name that may appear in the paper has been included only because it is essential to the contents of the paper.

Positions and opinions advanced in this paper are those of the author(s) and not necessarily those of SAE International. The author is solely responsible for the content of the paper.